Nonlinear damping of zonal modes in anisotropic weakly collisional trapped electron mode turbulence

R. Gatto
Università di Roma "Tor Vergata", 00133 Rome, Italy

P. W. Terry and D. A. Baver
University of Wisconsin-Madison, Madison, Wisconsin 53706

Comprehensive spectral analysis of a fluid model for trapped electron mode (TEM) turbulence reveals that marginally stable zonal modes at infinitesimal amplitude become robustly damped at finite amplitude. Zonal-mode structure, anisotropy, excitation, and wave number spectra are shown to result from interaction of the zero-frequency drift wave with the density advection nonlinearity. Heuristic dimensional balances, closure theory, and simulations manifest the primacy of the interaction, and yield energy transfer rates, fluctuation levels, spectra and finite-amplitude-induced dissipation. Strong sensitivity to the zero-frequency wave induces a marked spectral energy-transfer anisotropy that preferentially drives zonal modes relative to nonzonal modes. Zonal-mode excitation is accompanied by the nonlinear excitation of a spectrum of damped eigenmodes. The mixing of unstable TEM eigenmodes with the damped spectrum subjects zonal modes to finite-amplitude-induced damping. The combination of anisotropic transfer to zonal wave numbers and their nonlinear damping is shown to make this the dominant saturation mechanism for TEM turbulence. © *2006 American Institute of Physics*. [DOI: 10.1063/1.2167309]

I. INTRODUCTION

Recent work on nonlinear instability in a simple two-dimensional (2D) fluid model for trapped electron mode (TEM) turbulence[1] reveals that in addition to nonlinear instability there is also nonlinear damping in certain wave number ranges. Nonlinear damping is a dissipation of fluctuation energy with an amplitude-dependent rate. In TEM, unstable fluctuations at infinitesimal amplitude become energy sinks at finite amplitude. These fluctuations receive energy from conservative spectral transfer and dissipate it via nonlinear damping, shedding all vestiges of the linear instability. One spectrum subrange with such behavior is at low wave number extending to $k_y = 0$. Fourier modes with $k_y = 0$ are zonal modes in 2D. Zonal-mode wave numbers are marginally stable (undamped) at infinitesimal amplitude, but robustly damped at finite amplitude.[2] These results were found in a weakly collisional regime (collision rate ≪ diamagnetic frequency) that has historically been labeled as collisionless.

Nonlinear damping of zonal modes radically changes their dynamics and the turbulence that drives them. This article describes those changes. The changes are twofold. First, for TEM turbulence nonlinear damping of zonal modes saturates zonal-mode excitation, i.e., spectral energy transfer into zonal modes is balanced by nonlinear damping, allowing a steady state. Second, the spectral transfer to nonlinearly damped zonal modes is the dominant saturation channel for TEM instability-driven turbulence. It is dominant not just because the nonlinear damping rate is significant—slightly larger than the growth rate—or because nonlinearly damped zonal modes can be in close proximity to unstable modes in wave number space. It is dominant primarily because spectral transfer is highly anisotropic, with the energy transfer

rate to zonal modes significantly larger than the transfer rate to nonzonal modes. Consequently, if coupling to zonal modes is removed, the turbulence must avail itself of less efficient saturation channels, and the turbulence level rises markedly in order to balance the drive.

The importance of zonal flows in tokamak microturbulence was recognized from simulation results showing turbulence levels rising by an order of magnitude when zonal flows are artificially removed.[3–5] Zonal flows are thus believed to limit anomalous transport in tokamaks. Zonal flows are part of the fluctuation spectrum and couple to other fluctuations via three-wave coupling.[6] This has provided one avenue for inferring the presence of zonal modes in experiment[7,8] by means of the bicoherence or bispectrum, which quantifies the energy transfer rate between Fourier modes. Direct measurement of advecting flow has also identified a flow whose mean poloidal wave number is zero and bounded below $m = 3$,[9] and is part of the fluctuation spectrum near the frequency of the geodesic acoustic mode.[10]

Both the behavior and properties of zonal modes and the anisotropy of TEM turbulence arise from the interaction of waves and nonlinear advection. In TEM and other weakly collisional or collisionless systems, wave frequencies exceed instability growth rates. Saturation forces a balance between growth rate and nonlinearity, hence wave frequencies also exceed nonlinear decorrelation rates. This establishes a classic wave-dominated regime, like that of quasigeostrophic β-plane turbulence for scales larger than the Rhines radius.[11] In such regimes, fluctuation levels, spectrum shapes, and spectral transfer rates are subject to a balance, enforced at the zonal wave number, between wave frequency and nonlinearity. For this reason geophysical zonal flows reflect the anisotropy of the Rossby wave. Analysis of such regimes requires

proper treatment of wave frequencies. When there are multiple fields, time derivatives are combinations of multiple eigenfrequencies, and it is not proper to represent them by any single frequency (e.g., the frequency of the unstable mode). The simplest way to deal with this problem is to decompose the fields into their linear eigenmode constituents, recasting the model as nonlinear evolution equations for the eigenmode amplitudes.[1] This procedure is known as the helical decomposition in rotating fluids where the eigenmodes are helicity waves.[12,13] Here we apply a more generic label and refer to it as the eigenmode decomposition.

Two features are salient in the eigenmode decomposition. First, spectral energy transfer is anisotropic, with zonal modes receiving a disproportionate share. The enhancement occurs because $k_y = 0$ minimizes the difference of the linear eigenmode frequencies, which appears in the denominator of the mode coupling strength in the eigenmode decomposition. For zonal modes, the frequency difference vanishes to lowest order in the small parameter ν/ω_* (collision frequency/diamagnetic frequency), yielding the enhancement. Second, the coupling strength in the density advection nonlinearity is order (ν/ω_*) for the interaction of two Fourier modes on the unstable eigenmode branch, whereas it is order (ω_*/ν) for the interaction of the same two Fourier modes with one on the unstable eigenmode branch and one on the second eigenmode branch. The latter is damped for all wave numbers, is usually ignored in analyses because it is assumed to decay to zero, and does not even have a recognized label in the literature. However, simple parametric instability analysis shows that it is always excited in the linear growth phase. This eigenmode need only reach an amplitude two orders smaller than the amplitude of the unstable eigenmode for it to make order unity changes in the saturation dynamics. In fact, its amplitude is only one order smaller, and it dominates saturation. The excitation of this eigenmode, which we refer to simply as the damped eigenmode, means that there is a nonlinear eigenmode, given as an amplitude-dependent projection on the two linear eigenmodes of the basis set. It is shown here that any modification of the eigenmode of the linear instability produces damping of energy at the zonal wave number $k_y = 0$.

The relationship of zonal modes to wave physics in TEM puts it into a broad empirical similarity group characterized by anisotropic spectral condensation. Members of this group include Hasegawa-Mima turbulence,[14] TEM turbulence, quasigeostrophic β-plane turbulence, three-dimensional (3D) rotating turbulence,[15] and rotating stratified turbulence.[16] In each of these systems large-scale structure possessing the anisotropy of the zero-frequency *linear* wave is driven by isotropic nonlinearities in a wave-dominated regime. For Hasegawa-Mima, TEM, and quasigeostrophic β-plane turbulence, the global-scale structures are zonal flows and zonal density fields. For 3D rotating turbulence the structures are vortical columns. Introducing stratification allows the addition of layered zonal flow-like structures. Stable drift-wave and β-plane turbulence have nonlinearities that transfer energy to the global scales of zonal flows. In contrast, absent wave anisotropy, the nonlinearities of TEM and rotating and stratified turbulence drive energy to small scales away from

zonal flows. In these systems, near-resonant three wave interactions induce inverse transfer to large scales. This process, which violates the axiom that dynamical invariants govern cascade direction, has recently been described analytically and shown to satisfy a near-resonant wave-interaction condition.[17]

Nonlinear damping and the anisotropic wave-turbulence interaction are analyzed spectrally using strong turbulence statistical closure theory, dimensional analysis and numerical computation. We apply the closure to the eigenmode decomposition to obtain the energies of the unstable and damped eigenmodes, and the nonzero energy of the complex cross correlation of the two nonorthogonal eigenmodes. This task is accomplished analytically using weak collisionality as an expansion parameter, leading to expressions for the rms saturation values of the nonlinear eigenmode for both the turbulence and the zonal modes. From the dominant saturation balance it is clear that when the weak collisionality of the trapped electron scattering exceeds viscosity and small-scale collisional density diffusion, the turbulence saturates by energy transfer to the damped eigenmode, with the most significant channel being to the zonal modes. Kolmogorov-like energy transfer by forward cascading within the unstable eigenmode is subdominant, and has no effect on the saturation levels to lowest order. Dimensional analysis of the balance of wave frequency and nonlinearity at the zonal wave number in the eigenmode decomposition yields spectral densities for each of the eigenmode amplitudes.

This article is organized as follows. In Sec. II zonal mode excitation is described from the equations for the eigenmode decomposition and numerical computation. In Sec. III a comprehensive spectral picture of the saturated state of zonal modes and TEM turbulence is presented. Section IV deals with the nonlinear damping of zonal modes. Conclusions are given in Sec. V.

II. ZONAL MODE EXCITATION

TEM turbulence can be described by a simple fluid model, consisting of electron density and (ion) vorticity evolution equations that have been linked by quasineutrality. The model is

$$\frac{\partial n}{\partial t} - \nabla \phi \times z \cdot \nabla n + \nu(n - \phi) = -\hat{\alpha} v_D \frac{\partial \phi}{\partial y}, \tag{1}$$

$$\frac{\partial}{\partial t}(1 - \nabla^2 - \epsilon^{1/2})\phi - \epsilon^{1/2}\nu(n - \phi) + \nabla \phi \times z \cdot \nabla \nabla^2 \phi$$

$$= -v_D[1 - \epsilon^{1/2}\hat{\alpha}]\frac{\partial \phi}{\partial y}, \tag{2}$$

where $n = \epsilon^{1/2} n_e + \phi$ is an effective density, n_e is the density of trapped electrons, ϕ is the potential, $\epsilon^{1/2}$ is the trapping fraction, ν is the detrapping rate, v_D is the diamagnetic drift velocity, $\hat{\alpha} = 1 + 3\eta_e/2$, and η_e is the ratio of gradient scale lengths for the density and temperature. A derivation of this model and the dimensionless normalizations for n, ϕ, t, x, and y are given in Ref. 1. The quantity n will be referred to as the electron density, but it depends on the potential. Ap-

plying the spatial Fourier transform to Eqs. (1) and (2),

$$\frac{\partial n_k}{\partial t} + \nu n_k + [ik_y v_D \hat{\alpha} - \nu]\phi_k$$

$$= b_n(k) \equiv - \sum_{k'} (\mathbf{k}' \times \mathbf{z} \cdot \mathbf{k})\phi_{k'} n_{k-k'}, \qquad (3)$$

$$\frac{\partial \phi_k}{\partial t} - \frac{\epsilon^{1/2}\nu}{1 + k^2 - \epsilon^{1/2}}n_k + \frac{[ik_y v_D(1 - \hat{\alpha}\epsilon^{1/2}) + \nu\epsilon^{1/2}]}{1 + k^2 - \epsilon^{1/2}}\phi_k$$

$$= b_\phi(k) \equiv - \sum_{k'} \frac{(\mathbf{k}' \times \mathbf{z} \cdot \mathbf{k})(k - k')^2}{1 + k^2 - \epsilon^{1/2}}\phi_{k'}\phi_{k-k'}, \qquad (4)$$

where $b_n(k)$ is advection of turbulent electron density and $b_\phi(k)$ is advection of vorticity. Density advection has two spatial derivatives, vorticity advection has four. Consequently electron density advection is the dominant nonlinearity at large scales where $k \ll (\sqrt{n/\phi})_{\mathrm{rms}}$. Zonal flow spectra typically peak at low k_x, putting the energy containing zonal-flow scales in the long wavelength regime. Thus while zonal mode excitation is conventionally associated with the Reynolds stress and flows, density advection and density zonal modes must be considered to form an accurate picture of the physics. Recent analysis of data from the Texas experimental tokamak infers the excitation of zonal flows through bispectra of coupled density and electrostatic potential fluctuations,[8] consistent with density advection. Advective nonlinearities of density or pressure have historically been identified with energy transfer to small scales. Hence the physics of spectral transfer to the long wavelengths of zonal flows[17] is as nontrivial as it is vital to zonal flow formation.

Because zonal modes are not linearly unstable, they reach finite amplitude only by spectral transfer from modes with $k_y \neq 0$. The process is highly sensitive to wave anisotropy. The physics can be understood heuristically. In the weakly collisional regime the growth rate is smaller than the wave frequency ($\gamma \propto \nu \ll \omega \propto k_y v_D$). At saturation the nonlinearities must become as large as the growth rate to achieve stationarity, but these remain smaller than wave frequencies. In such wave-dominated regimes, frequencies enter dominant balances through their role in the turbulent decorrelation rate. However the wave frequency vanishes for $k_y = 0$. This leads to a singular layer in wave number space in which spectral transfer to $k_y = 0$ becomes sufficiently large to enable the spectrum at $k_y = 0$ to compensate for the vanishing of k_y. This was first demonstrated numerically for quasigeostrophic β-plane turbulence.[11] (There, the labeling of x and y axes is opposite to the plasma convention, and the wave term vanishes for $k_x = 0$). A steep k_y^{-5} spectrum develops for wave numbers near $k_x = 0$ to keep the wave terms in balance with the nonlinearity. The spectral density outside the band near $k_x = 0$ is much smaller, falling off as $k^{-5/3}$. The steep spectrum feature, which represents a geophysical zonal flow, is created by highly anisotropic spectral transfer, favoring $k_x = 0$ zonal modes over other nonzonal modes.

The situation is analogous to the singular layers that arise in partial differential equations whenever the term of the highest-order derivative can drop out of a dominant balance because of the smallness of a multiplicative coefficient.

The term remains in the balance if the highest derivative becomes large enough to offset the small coefficient. In partial differential equations the term with the highest derivative dictates the singularity. In spectral equations the term with the lowest power of k dictates the singularity (i.e., the wave term) because it dominates at long wavelengths. This term vanishes for $k_y = 0$, hence the singularity is expressed as an enhancement of spectral density and spectral transfer for $k_y = 0$.

This anisotropic enhancement is readily evident in the eigenmode decomposition. This transformation is a nonlinearly evolving projection onto the basis set formed by the linear eigenmodes. Under the eigenmode decomposition the density and potential are written as

$$\begin{pmatrix} n_k(t) \\ \phi_k(t) \end{pmatrix} = \beta_1(k,t)\begin{pmatrix} R_1 \\ 1 \end{pmatrix} + \beta_2(k,t)\begin{pmatrix} R_2 \\ 1 \end{pmatrix}$$

$$= \begin{pmatrix} R_1 & R_2 \\ 1 & 1 \end{pmatrix}\begin{pmatrix} \beta_1(k,t) \\ \beta_2(k,t) \end{pmatrix}$$

$$\equiv \mathbf{M}\begin{pmatrix} \beta_1(k,t) \\ \beta_2(k,t) \end{pmatrix}, \qquad (5)$$

where $\beta_1(k,t)$ and $\beta_2(k,t)$ are the instantaneous (nonlinearly evolving) amplitudes of the linear eigenmodes, and $[R_1, 1]$ and $[R_2, 1]$ are the eigenvectors. The components $R_j(k)$ are the ratio n_k/ϕ_k for each eigenfrequency ω_j, and are obtained by linearizing Eq. (4), replacing $\partial/\partial t$ with $-i\omega_j$, and solving for n_k. The result is

$$R_j(k) = -\frac{1 + k^2 - \epsilon^{1/2}}{\nu\epsilon^{1/2}}\left[i\omega_j - \frac{ik_y v_D(1 - \hat{\alpha}\epsilon^{1/2}) + \nu\epsilon^{1/2}}{1 + k^2 - \epsilon^{1/2}}\right], \qquad (6)$$

where the eigenfrequencies ω_j are the roots of the characteristic equation,

$$\omega^2(1 + k^2 - \epsilon^{1/2}) + \omega[-v_D k_y(1 - \hat{\alpha}\epsilon^{1/2}) + i\nu(1 + k^2)]$$
$$- ik_y v_D \nu = 0. \qquad (7)$$

Evolution equations for $\beta_j(k,t)$ are obtained by inverting Eq. (5), taking a time derivative, using Eqs. (3) and (4) to write $\dot{n}_k$ and $\dot{\phi}_k$ in terms of their evolution operators, and rewriting n_k and ϕ_k in terms of $\beta_1(k)$ and $\beta_2(k)$ with Eq. (5). The result is a pair of equations that are diagonal in the linear coupling but mix the two nonlinearities,

$$\begin{pmatrix} \dot{\beta}_1(k) \\ \dot{\beta}_2(k) \end{pmatrix} + \begin{pmatrix} i\omega_1 & 0 \\ 0 & i\omega_2 \end{pmatrix}\begin{pmatrix} \beta_1(k) \\ \beta_2(k) \end{pmatrix}$$

$$= \frac{1}{R_1(k) - R_2(k)}\begin{pmatrix} b_n - R_2(k)b_\phi \\ -b_n + R_1(k)b_\phi \end{pmatrix}, \qquad (8)$$

where b_n and b_ϕ are understood to be evaluated using the substitution $n_k = R_1\beta_1 + R_2\beta_2$ and $\phi_k = \beta_1 + \beta_2$. A useful approximation to Eq. (8), one that will be the basis of analysis in subsequent sections, is given by

$$\dot{\beta}_j(k) + i\omega_j\beta_j(k) \approx \sum_{k'} \frac{(-1)^j (\mathbf{k}' \times \mathbf{z} \cdot \mathbf{k})}{R_1(k) - R_2(k)} [R_1(k')\beta_1(k')$$

$$+ R_2(k')\beta_2(k')]\beta_1(k-k'). \quad (9)$$

This approximation is reached by discarding the vorticity advection nonlinearity b_ϕ and assuming that $\beta_2 \ll \beta_1$, so that β_2 can be dropped relative to β_1. These approximations conserve energy and are generally valid in the long wavelength regime.

The strong anisotropy of spectral transfer favoring zonal modes is readily evident in the behavior of the factor $(R_1 - R_2)^{-1}$ in Eq. (8). From Eq. (6), this factor is controlled by the eigenfrequency difference $\omega_1(k) - \omega_2(k)$:

$$\frac{1}{R_1(k) - R_2(k)} = \left(\frac{i\nu\epsilon^{1/2}}{1 + k^2 - \epsilon^{1/2}} \right) \frac{1}{[\omega_1(k) - \omega_2(k)]}. \quad (10)$$

The eigenmode frequencies are the roots of Eq. (7). The first root ω_1 is the unstable weakly collisional trapped electron mode. For $k_y \neq 0$ it has a real frequency proportional to $v_D k_y$ and a growth rate proportional to ν. For $k_y = 0$ this root has $\omega_1 \equiv 0$. If the nonzonal modes are weakly collisional, $\nu < v_D k_y$, the frequency for nonzonal and zonal wave numbers is

$$\omega_1(k) = \frac{v_D k_y (1 - \hat{\alpha}\epsilon^{1/2})}{(1 + k^2 - \epsilon^{1/2})} + \frac{i\nu\epsilon^{1/2}[\hat{\alpha}(1 + k^2) - 1]}{(1 + k^2 - \epsilon^{1/2})(1 - \hat{\alpha}\epsilon^{1/2})}$$

$$+ O\left(\frac{\nu^2}{v_D k_y} \right) \quad (k_y \neq 0), \quad (11)$$

$$\omega_1(k) = 0 \quad (k_y = 0). \quad (12)$$

The second root ω_2 is a stable eigenmode branch. Its frequency for nonzonal and zonal wave numbers is

$$\omega_2(k) = \frac{-i\nu}{(1 - \hat{\alpha}\epsilon^{1/2})} - \frac{\nu^2\epsilon^{1/2}[\hat{\alpha}(1 + k^2) - 1]}{k_y v_D (1 - \hat{\alpha}\epsilon^{1/2})^3}$$

$$+ O\left(\frac{\nu^3}{v_D^2 k_y^2} \right) \quad (k_y \neq 0), \quad (13)$$

$$\omega_2(k) = \frac{-i\nu(1 + k_x^2)}{1 + k_x^2 - \epsilon^{1/2}} \quad (k_y = 0). \quad (14)$$

In comparing $\omega_1(k) - \omega_2(k)$ for $k_y = 0$ and $k_y \neq 0$ we observe that the vanishing of $\omega_1(k)$ for $k_y = 0$ makes this difference $O(v_D k_y)$ for $k_y \neq 0$ and $O(\nu)$ for $k_y = 0$. Therefore, the mode-coupling-strength factor $[R_1(k) - R_2(k)]^{-1}$ goes as

$$\frac{1}{R_1(k) - R_2(k)} = \begin{cases} \dfrac{i\nu\epsilon^{1/2}}{k_y v_D (1 - \hat{\alpha}\epsilon^{1/2})} & \text{for } k_y \neq 0 \\[2ex] \dfrac{\epsilon^{1/2}}{1 + k_x^2} & \text{for } k_y = 0. \end{cases} \quad (15)$$

The difference in coupling strengths between triplets in which $\mathbf{k}$ is a zonal wave vector versus those in which it is not carries directly over to spectral transfer rates, which derive from second order moments of Eq. (9). The anisotropy of the coupling factor $(R_1 - R_2)^{-1}$ indicates that the rate of energy transfer into zonal modes is larger by a factor $\bar{k}_y v_D / \nu$ than it
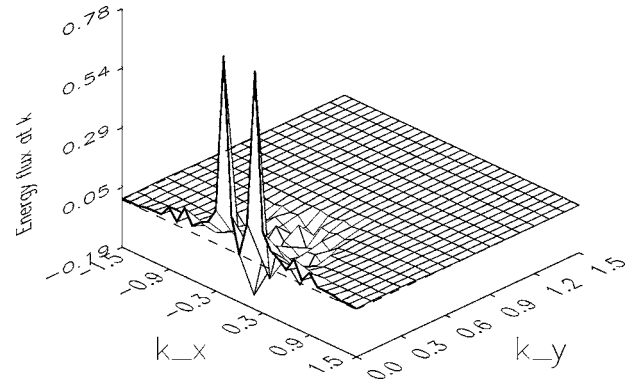

FIG. 1. Spectral distribution of energy flux, time-averaged in the saturation phase. The largest flux values are for zonal modes.

is for transfer into nonzonal modes. The anisotropy of spectral transfer is illustrated in Fig. 1, which plots the spectral transfer rate as a function of k_x and k_y from numerical steady state solutions of Eqs. (1) and (2). The large peaks at the edge of the wave number plane represent energy transferred into zonal modes. The rate of transfer is significantly larger than that of nonzonal modes.

The evolution equation in the eigenmode decomposition, Eq. (8), also clearly reveals that the stable eigenmode is excited. As the system evolves from infinitesimal amplitudes the nonlinearity grows because each of its two β_1 factors exponentiates. Eventually the nonlinearity saturates the instability by balancing the linear growth term $-i\omega_1\beta_1$, which itself is growing. However, well before, the same nonlinearity overwhelms the damping term of the β_2 equation, $-i\omega_2\beta_2$, which initially decreases exponentially. The result is exponential growth of β_2. In Sec. IV we will show that the excitation of the damped eigenmode directly leads to nonlinear damping of zonal modes.

Zonal modes are excited in precisely the same way the damped eigenmode is excited, but as shown above, are driven harder by virtue of the anisotropy of the mode coupling factor $[R_1(k) - R_2(k)]^{-1}$. The initial nonlinear-growth phase of both the damped eigenmode, and of zonal modes on both branches, can be described analytically by noting that the exponentially growing β_1-field dominates the nonlinearity, allowing the nonlinear term that depends on β_2 to be dropped. Thus, Eq. (8) can be written

$$\begin{pmatrix} d/dt + i\omega_1 & 0 \\ 0 & d/dt + i\omega_2 \end{pmatrix} \begin{pmatrix} \beta_1(k) \\ \beta_2(k) \end{pmatrix}$$

$$= \frac{1}{R_1(k) - R_2(k)} \begin{pmatrix} 1 \\ -1 \end{pmatrix} \sum_{k'} \frac{(\mathbf{k}' \times \mathbf{z} \cdot \mathbf{k})}{2}$$

$$\times [R_1(k') - R_2(k-k')]\beta_1(k',t)\beta_1(k-k',t), \quad (16)$$

where the long wavelength regime with $b_n > R_2 b_\phi$ has been assumed. Before saturation, $\beta_1(k',t)$ and $\beta_1(k-k',t)$ grow exponentially $(k_y - k_y', k_y' \neq 0)$ yielding,

$$\beta_1(k',t) = \beta_1(k',t=0)\exp[-i\omega_1(k')t] \quad (k_y' \neq 0). \quad (17)$$

and a similar expression for $\beta_1(k-k',t)$. Consider first nonzonal β_2 eigenmodes. The linear term of the β_2 equation first
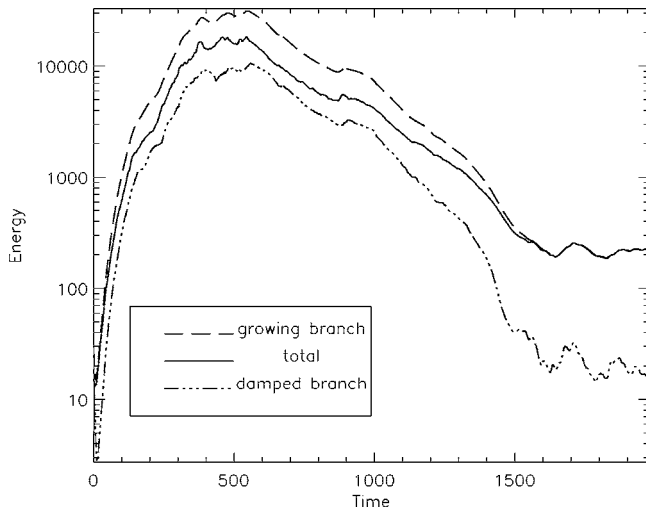
FIG. 2. Time evolution of the total energy and the energies in the growing and damped eigenmodes.

FIG. 3. Time evolution of the total energy, zonal mode energy, and nonzonal mode energy.

decays exponentially, allowing the nonlinearity to dominate long before saturation. Once that happens, but before β_2 becomes large enough to contribute to the nonlinearity, or for the linear term to balance the nonlinearity, the evolution of β_2 is governed by the nonlinearity of Eq. (16), with $\beta_1(k',t)$ and $\beta_1(k-k',t)$ approximated as in Eq. (17). It is straightforward to integrate the nonlinearity to obtain

$$\beta_2(k,t) = \sum_{k'} \frac{(\mathbf{k}' \times \mathbf{z} \cdot \mathbf{k})}{2(1-\epsilon^{1/2}\hat{\alpha})^2} \frac{\nu}{k_y v_D} \left[i\hat{\alpha}\epsilon^{1/2} 2\mathbf{k} \cdot (\mathbf{k}' - \mathbf{k}) \right.$$
$$\left. - \frac{\nu(\hat{\alpha}-1)(1-\epsilon^{1/2})(2k_y'-k_y)}{k_y' v_D(k_y-k_y')(1-\epsilon^{1/2}\hat{\alpha})^2} \right]$$
$$\times \beta_1(k',t=0)\beta_1(k-k',t=0)$$
$$\times \frac{\exp[-i\omega_1(k')t - i\omega_1(k-k')t]}{i[\omega_2(k) - \omega_1(k') - \omega_1(k-k')]}. \quad (18)$$

This expression is valid for turbulent modes on the damped branch until β_2 is sufficiently large to contribute to nonlinear evolution or saturate the instability. The exponential factor contains a sum of growth rates of modes k' and $k-k'$, allowing the damped branch to grow exponentially at a rate that exceeds the growth rate of the unstable branch. This behavior is evident in Fig. 2, which shows the time evolution of the energies in the growing and damped branches. It is also evident that the damped branch begins growing exponentially long before saturation of the instability.

The assumptions made in deriving Eq. (18) apply equally well to zonal modes on both the unstable and damped branches. On the damped branch, zonal modes decay initially until the nonlinearity dominates. On the unstable branch the nonlinearity dominates at all times because $\omega_1 = 0$ makes the linear term zero. Consequently the evolution of β_1 and β_2 for $k_y=0$ is similar to that of Eq. (18), except that in deriving the evolution, the factor $(R_1-R_2)^{-1}$ must be taken from the second line of Eq. (15) instead of the first. The evolution of zonal modes in either eigenmode branch is given by
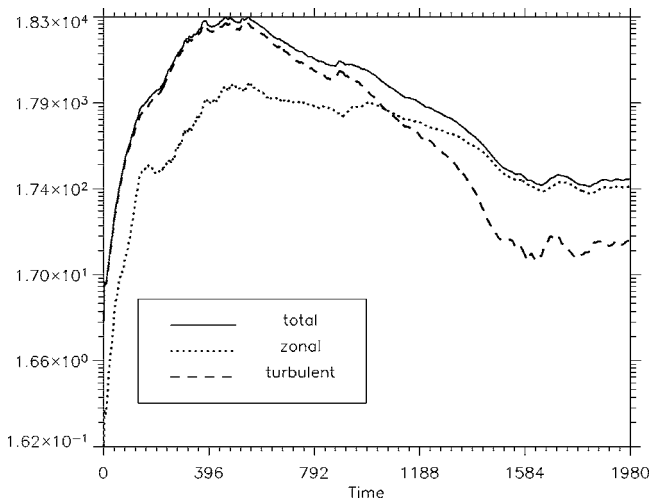
$$\beta_j(k_x,t) = \sum_{k'} \frac{(-1)^j k_y' k_x \epsilon^{1/2}}{2(1-\epsilon^{1/2}\hat{\alpha})} \left[\hat{\alpha} k_x(2k_x'-k_x) \right.$$
$$\left. - \frac{2i\nu(\hat{\alpha}-1)(1-\epsilon^{1/2})}{k_y' v_D(1-\epsilon^{1/2}\hat{\alpha})^2} \right]$$
$$\times \beta_1(k',t=0)\beta_1(k-k',t=0)$$
$$\times \left. \frac{\exp[-i\omega_1(k')t - i\omega_1(k-k')t]}{i[\omega_2(k) - \omega_1(k') - \omega_1(k-k')]} \right|_{k_y=0}. \quad (19)$$

The nonlinear evolution of zonal-mode energy is shown in Fig. 3. Note that the initial exponential growth is similar to that of the damped eigenmode. The growth of zonal modes under nonlinear coupling has been analyzed previously, although frequently for limited spectral interactions (e.g., a single zonal mode with two turbulent sideband modes), or with implicit scale separation assumptions, and not accounting for the accompanying excitation of damped eigenmodes. The early phase of zonal mode excitation is well approximated by weak turbulence approximations like those used in deriving Eq. (19). However, weak turbulence theory breaks down at saturation. Further description of the turbulence must not only utilize strong turbulence theory, but must account for the finite amplitude of the damped eigenmode. This matter will be taken up in the next section. Damped eigenmodes, specifically the geodesic acoustic mode, have been observed in the context of zonal flows.[9]

III. SATURATION ANALYSIS

In systems like TEM that develop a nonlinear eigenmode, an analytic description of the eigenmode in the saturated state can be obtained by solving the equations for the eigenmode decomposition. If the turbulence is stationary this generally entails finding stationary eigenmode energies. The physics of zonal modes can be investigated by examining important spectral properties for the zonal-mode wave number $k_y=0$, and comparing to nonzonal modes. Properties of

interest include energy transfer, dissipation, and energy levels, and are explored in the next two sections.

Saturation in the eigenmode decomposition entails the balance of linear instability or damping with nonlinear transfer terms. This same approach, of course, is invariably applied to models of basic field evolution (i.e., density, potential, etc.). However its application to basic fields is not valid if a nonlinear eigenmode develops. The drives and damping of different eigenmodes are mixed in proportions that depend on fluctuation level and cannot be determined from any balance within the basic-field representation. Direct balances of linear drive and nonlinearity are intrinsically valid in the eigenmode decomposition. However the nonlinearities are mixed, and the energy path from source to sink is not confined within a single eigenmode. In TEM turbulence, energy goes from the instability (Im ω_1) to $|\beta_1|^2$, then to Im$\langle \beta_1^* \beta_2 \rangle$, and finally to Re$\langle \beta_1^* \beta_2 \rangle$ and $|\beta_2|^2$. The damping of the last three quantities by Im ω_2 is the sink that saturates the turbulence. Because the eigenmodes are nonorthogonal, the total energy is a combination of $|\beta_1|^2$, $|\beta_2|^2$, Im$\langle \beta_1^* \beta_2 \rangle$, and Re$\langle \beta_1^* \beta_2 \rangle$. Consequently the dissipation of total energy, both

negative (instability drive) and positive (damping), is not given by any single eigenmode growth rate, but by an amplitude-dependent combination. Solution of the eigenmode decomposition equations allows calculation of the energy dissipation rate. This is detailed in the next section.

The evolution equations for the energies $|\beta_1|^2$, $|\beta_2|^2$, Im$\langle \beta_1^* \beta_2 \rangle$, and Re$\langle \beta_1^* \beta_2 \rangle$ are written out in Ref. 1 as Eqs. (32)–(34). Equation (34) is complex, with independent real and imaginary parts, hence there are four equations that determine the four energies. We do not rewrite the four evolution equations here because of their length. However, they are the basis for analysis of saturation. The original saturation analysis of Ref. 1 considered balances involving nonzonal modes only, i.e., it treated saturation and spectral transfer as essentially isotropic. It also assumed long wavelengths ($k^2 < 1$), but did not formally order k^2 under the expansion for $\nu/v_D k_y \ll 1$. The object of this section is to account for the anisotropy of spectral transfer and document its effect on energy levels and spectra. The ordering adopted for $k^2 < 1$ is $k^2 = O(\nu/v_D k_y)^2$. To illustrate our analysis of anisotropy, we consider Eq. (32) of Ref. 1 in detail. This equation is

$$\frac{\partial}{\partial t}|\beta_1|^2 = 2 \, \mathrm{Im} \, \omega_1 |\beta_1|^2 + \mathrm{Re}\sum_{k'} \left\{ \frac{1}{2} \frac{C_1(k,k')}{(i\omega_1' + i\omega_1'' - i\omega_1^* - \Delta\omega_1' - \Delta\omega_1'' - \Delta\omega_1^*)} [C_1(k',k) \, |\beta_1''|^2|\beta_1|^2 + C_1(k'',k)|\beta_1'|^2|\beta_1|^2 + C_1^*(k,k') \right.$$

$$\times |\beta_1'|^2|\beta_1''|^2 + C_2(k',-k'')|\beta_1|^2\langle \beta_1'' \beta_2''^* \rangle + C_2(k',k)|\beta_1''|^2\langle \beta_1^* \beta_2 \rangle + C_2(k'',k)|\beta_1'|^2\langle \beta_1^* \beta_2 \rangle + C_2(k'',-k')|\beta_1|^2\langle \beta_1' \beta_2'^* \rangle$$

$$+ C_2^*(k,k')|\beta_1''|^2\langle \beta_1' \beta_2'^* \rangle + C_2^*(k,k'')|\beta_1'|^2\langle \beta_1'' \beta_2''^* \rangle + \frac{C_2(k,k')}{(i\omega_2' + i\omega_1'' - i\omega_1^* - \Delta\omega_2' - \Delta\omega_1'' - \Delta\omega_1^*)} [C_1(k'',k)|\beta_1|^2\langle \beta_1'^* \beta_2' \rangle$$

$$- C_1(k',k)|\beta_1''|^2|\beta_1|^2 + C_1^*(k,k')|\beta_1'|^2\langle \beta_1'^* \beta_2' \rangle + C_2(k'',k)\langle \beta_1'^* \beta_2' \rangle\langle \beta_1^* \beta_2 \rangle + C_2(k'',-k')|\beta_1|^2|\beta_2'|^2 - C_2(k',k)$$

$$\times |\beta_1''|^2\langle \beta_1^* \beta_2 \rangle - C_2(k',-k'')|\langle \beta_1'' \beta_2''^* \rangle|\beta_1|^2 + C_2^*(k,k')|\beta_1''|^2|\beta_2'|^2 + C_2^*(k,k'')\langle \beta_1'' \beta_2''^* \rangle|\langle \beta_1'^* \beta_2' \rangle] \right\}, \qquad (20)$$

where

$$C_1(k,k') = - (\mathbf{k'} \times \mathbf{z} \cdot \mathbf{k}) \frac{R_1(k') - R_1(k'')}{R_1(k) - R_2(k)}, \qquad (21)$$

$$C_2(k,k') = - (\mathbf{k'} \times \mathbf{z} \cdot \mathbf{k}) \frac{R_2(k')}{R_1(k) - R_2(k)}, \qquad (22)$$

are coupling strengths, and we use the shorthand notation $\beta_j = \beta_j(k)$, $\beta_j' = \beta_j(k')$, $\beta_j'' = \beta_j(k-k')$, $\omega = \omega(k)$, $\omega' = \omega(k')$, and $\omega'' = \omega(k-k')$. The frequencies $\Delta\omega_1$ and $\Delta\omega_2$ are complex amplitude-dependent eddy damping rates, given in Eqs. (35) and (36) of Ref. 1. The $|\beta_1|^2$ evolution equation written in this article as Eq. (20) and the three other coupled energy evolution equations are too complicated to permit a general analytic solution. However it is possible to determine how the solution scales with the instability parameters ν and $v_D k_y$. The scalings can be found using asymptotic analysis for $\nu/v_D k_y \ll 1$ under the ansatz that both the instability drive, Im ω_1, and the stable eigenmode damping, Im ω_2, remain in

dominant balances. From Fig. 1, it is evident that this ansatz is operative in numerical solutions, particularly the requirement that Im ω_2 enter the dominant balance.

To document the effects of anisotropy we find the solution of the anisotropic energy evolution equations and compare it with the previous solution that assumed isotropy. The asymptotic analysis requires the expansion of C_1, C_2, and the turbulent three-wave decorrelation rates $iW_{jmn} = i\omega_j' + i\omega_m'' - i\omega_n^* - \Delta\omega_j' - \Delta\omega_m'' - \Delta\omega_n^*$ for $\nu/v_D k_y \ll 1$. The isotropic solution was found using expansions of C_1, C_2, and iW_{jmn} that assumed k_y, k_y', $k_y - k_y' \neq 0$. It emerged from an asymptotically consistent balance with the leading order energy scalings as

$$|\beta_1|^2 \sim A_1 \frac{v_D^2 \overline{k_y^2}}{\overline{k^4}},$$

$$|\beta_2|^2 \sim A_2 \frac{\nu^2}{\bar{k}^4},$$

$$\text{Re}\langle\beta_1^*\beta_2\rangle \sim A_r \frac{\nu^2}{\bar{k}^4}, \tag{23}$$

$$\text{Im}\langle\beta_1^*\beta_2\rangle \sim A_i \frac{\nu v_D \bar{k}_y}{\bar{k}^4},$$

where the energies are spectrum averaged, $\bar{k}_y$ is a mean poloidal wave number, and $\bar{k}^4$ is a mean fourth power of wave number generated from spectrum averages of $(\mathbf{k}' \times \mathbf{z} \cdot \mathbf{k})^2$. In the leading order balance of Eq. (20), the only nonlinear terms that enter are those proportional to $C_2(k,k')C_2(k',k)|\beta_1''|^2\langle\beta_1^*\beta_2\rangle$ and $C_2(k,k')C_2(k',-k'')|\beta_1|^2\langle\beta_1''^*\beta_2''\rangle$. Both of these terms involve coupling between a wave at k' on the damped branch and waves at k and k'' on the unstable branch. This indicates that transfer to the damped branch through the cross correlation $\text{Im}\langle\beta_1^*\beta_2\rangle$ plays a prominent role in saturation. The Kolmogorov-like saturation channel that involves transfer to higher-k Fourier modes within the growing eigenmode branch is subdominant. (This involves the isotropic part of terms in the $|\beta_1|^2$ equation that depend only on C_1 and β_1.)

Anisotropy arises because $\omega_1 \sim k_y v_D$ is large and finite for $k_y \neq 0$, whereas $\omega_1=0$ for $k_y=0$. This in turn affects C_1 and C_2 through Eq. (15), and iW_{jmn}. Because the wave numbers k, k', and $k-k'$ appear in different combinations as the arguments of C_1 and C_2 in Eq. (20), anisotropic transfer is tracked by considering the limits $k_y \to 0$ and $k_y' \to 0$. The limit $k_y-k_y' \to 0$ reproduces terms already generated by $k_y' \to 0$ and need not be tracked for scaling analysis. There are two types of anisotropic interactions. One is the interaction of zonal modes with $k_y=0$ and nonzonal modes with $k_y' \neq 0$. (The nonlinear coupling vanishes for a zonal modes directly interacting with another zonal mode.) The other is the interaction of nonzonal modes with $k_y \neq 0$ and zonal modes with $k_y'=0$. For scaling analysis that does not resolve the full spectral variation there are now eight quantities to be found from the asymptotic balances. These are $|\beta_1|^2$, $|\beta_2|^2$, $\text{Re}\langle\beta_1\beta_2^*\rangle$, and $\text{Im}\langle\beta_1\beta_2^*\rangle$ for $k_y=0$ and the same quantities for $k_y \neq 0$. Likewise, there are eight balance equations obtained by taking $k_y=0$ and $k_y \neq 0$ in Eqs. (32)–(34) of Ref. 1. Table I summarizes the asymptotic scalings of C_1, C_2, and iW_{jmn} in the small parameter $\delta=\nu/v_D\bar{k}_y$ for k_y and k_y' values corresponding to zonal and nonzonal modes.

Using the leading order scalings indicated in Table I, there is a consistent leading order balance in all eight energy evolution equations if the energies at nonzonal wave numbers have the same scalings as the isotropic analysis [Eq. (23)], and the zonal energies have the scalings

$$|\beta_1(k_x, k_y=0)|^2 \sim A_{1Z} \frac{v_D^2 \bar{k}_y^2}{\bar{k}^4},$$

TABLE I. Leading order scalings of the coupling strengths and decorrelation rates appearing in the energy evolution equations, where $\delta=\nu/v_D\bar{k}_y$.

	$k_y, k_y' \neq 0$	$k_y=0$	$k_y'=0$
$C_1(k,k')$	$O(\delta^2)+iO(\delta^3)$	$iO(\delta)+O(\delta^2)$	$iO(\delta)+O(\delta^2)$
$C_1(k'',k)$	$O(\delta^2)+iO(\delta^3)$	$iO(\delta)+O(\delta^2)$	$iO(\delta)+O(\delta^2)$
$C_1(k',k)$	$O(\delta^2)+iO(\delta^3)$	$iO(\delta)+O(\delta^2)$	$iO(\delta)+O(\delta^2)$
$C_2(k,k')$	$O(1)+iO(\delta)$	$iO(\delta^{-1})+O(1)$	$iO(\delta)+O(\delta^2)$
$C_2(k,k'')$	$O(1)+iO(\delta)$	$iO(\delta^{-1})+O(1)$	$O(1)+iO(\delta)$
$C_2(k',k)$	$O(1)+iO(\delta)$	$iO(\delta)+O(\delta^2)$	$iO(\delta^{-1})+O(1)$
$C_2(k'',k)$	$O(1)+iO(\delta)$	$iO(\delta)+O(\delta^2)$	$O(1)+iO(\delta)$
$C_2(k',-k'')$	$O(1)+iO(\delta)$	$O(1)+iO(\delta)$	$iO(\delta^{-1})+O(1)$
$C_2(k'',-k')$	$O(1)+iO(\delta)$	$O(1)+iO(\delta)$	$iO(\delta)+O(\delta^2)$
iW_{111}	$\nu[O(1)+iO(\delta)]$	$\nu[O(1)+iO(\delta)]$	$\nu[O(1)+iO(\delta)]$
iW_{211}	$iv_D\bar{k}_y[O(1)+iO(\delta)]$	$iv_D\bar{k}_y[O(1)+iO(\delta)]$	$\nu[O(1)+iO(\delta)]$
iW_{112}	$iv_D\bar{k}_y[O(1)+iO(\delta)]$	$\nu[O(1)+iO(\delta)]$	$iv_D\bar{k}_y[O(1)+iO(\delta)]$
iW_{212}	$iv_D\bar{k}_y[O(1)+iO(\delta)]$	$iv_D\bar{k}_y[O(1)+iO(\delta)]$	$iv_D\bar{k}_y[O(1)+iO(\delta)]$

$$|\beta_2(k_x, k_y=0)|^2 \sim A_{2Z} \frac{v_D^2 \bar{k}_y^2}{\bar{k}^4},$$

$$\text{Re}\langle\beta_1^*(k_x, k_y=0)\beta_2(k_x, k_y=0)\rangle \sim A_{rZ} \frac{v_D^2 \bar{k}_y^2}{\bar{k}^4}, \tag{24}$$

$$\text{Im}\langle\beta_1^*(k_x, k_y=0)\beta_2(k_x, k_y=0)\rangle \sim A_{iZ} \frac{\nu v_D \bar{k}_y}{\bar{k}^4}.$$

With these scalings the dominant balances are markedly different when anisotropy is accounted for versus when isotropy is assumed. Whereas only two of the eighteen nonlinear terms entered the dominant balance of the isotropic analysis, all eighteen terms enter the dominant balance of Eq. (20) with $k_y \neq 0$ but $k_y'=0$ allowed in the spectrum sums. Consequently, accounting for the coupling to zonal modes results in nearly a factor of 10 increase in the saturation channels available to absorb the energy injected into the turbulence by the instability. This increase in saturation channels is consistent with Fig. 1, which showed that most of the energy provided by the instability flows to the zonal modes.

The spectral transfer described above occurs in a 3D space having k_x and k_y as two dimensions, and the third as the two discrete states of *eigenmode space*. This 3D space is visualized as two parallel k_x-k_y planes, one for each eigenmode. Spectral transfer terms in Eq. (20) fall into four categories. The first is isotropic flow to large wave number occurring in the k_x-k_y plane of the unstable eigenmode, and is governed by the first three terms of Eq. (20) with $k_y, k_y' \neq 0$. These same three terms with $k_y'=0$ describe anisotropic flow within the plane of the unstable eigenmode from unstable Fourier modes to zonal modes, and comprise the second category. The third category consists of terms like $C_2(k,k')C_2(k',k)|\beta_1''|^2\langle\beta_1^*\beta_2\rangle$ that transfer energy isotropically in wave number space but jump from the unstable eigenmode plane to the stable eigenmode plane. The fourth category consists of terms like $C_2(k,k')C_2(k',k)|\beta_1''|^2\langle\beta_1^*\beta_2\rangle$

with $k_y'=0$. These also jump planes, but the transfer in k space is anisotropic to $k_y'=0$. Of these four categories, only the first can be labeled Kolmogorov-like. The third and fourth involve the stable eigenmode. The second represents inverse transfer in a nonlinearity historically identified with forward transfer. The ratio of the three Kolmogorov-like terms to any rate in the other three categories is obtained by substituting Eqs. (23) and (24) into the terms in question. In all cases the ratio is $\nu^2/v_D^2\bar{k}_y^2$, and is truly small. Moreover, there are 3 terms in the second category, 2 in the third category, and 15 in the fourth category, all of the same order. This quantifies the assertion that the instability saturates by non-Kolmogorov-like transfer, and that transfer is overwhelmingly anisotropic and primarily to modes on the stable branch. Non-Kolmogorov-like saturation via spectral transfer to longer toroidal wavelengths has been observed in simulation of electron temperature gradient turbulence.[18] Because eigenmode space was not resolved, it is not clear if this transfer involves a single eigenmode or multiple branches.

The change in scaling of $|\beta_2|^2$ and $\langle\beta_1^*\beta_2\rangle$ in the anisotropic analysis relative to the isotropic analysis is also noteworthy. It suggests that the zonal modes in these quantities have larger levels than the nonzonal modes and that there is therefore significantly more damping in the system than if the coupling to zonal modes is removed. In the next section we show that the nonlinear eigenmode created by the excitation of the both the unstable and damped eigenmodes is robustly damped for zonal wave numbers. The zonal modes are therefore an energy sink. Because transfer to zonal modes dominates the Kolmogorov transfer to damped modes at higher wave number this is the saturation mechanism for the instability. Consequently, there is a change in the saturation level of nonzonal modes that follows from the inclusion or exclusion of the anisotropic saturation channels to zonal modes. This change is illustrated in Fig. 4. The fluctuation level increases by an order of magnitude when the coupling to zonal modes is removed. It must therefore be concluded that in this system it is the nonlinear damping of zonal modes that leads to the lower saturation level when zonal modes are present. Although results like these have been exhibited since zonal flows were first examined in unstable fusion plasmas, we emphasize that, in light of the previous discussion, the interpretation of these results is quite different from the one usually given. Here zonal modes reduce saturation because they are the dominant sink of fluctuation energy through a finite amplitude-induced damping mechanism. In contrast, the commonly invoked mechanism of zonal flow shearing[19] derives from differential advection and is not intrinsically dissipative.

The differences between this and other models are also illustrated by the scaling of saturation level with zonal flow damping. In simulations of ion temperature gradient turbulence the saturation level increases with zonal-flow damping rate. Here, $|\beta_2|^2\sim\nu^2$, but $|\beta_1|^2\sim\nu^0$. Although the damped-eigenmode level increases with larger zonal flow damping (which is proportional to ν), the level of the unstable eigenmode does not. However, in this model, unlike others, a single dissipative parameter ν controls both the instability

free energy (growth rate) and the energy sink that saturates the instability. Moreover the sink is only accessed as a finite-amplitude effect through excitation of the damped eigenmode. Recent work shows that damped eigenmodes affect saturation under certain conditions governed by the linear and nonlinear coupling, conditions that may not be met in all models.[20] These differences are implicated in cases where there is little change in fluctuation level when the coupling to zonal flows is removed,[21] because in those cases there is little deviation from the state of the linear instability.

Zonal mode spectra can be derived for β_1 and β_2 using the procedure validated in Ref. 11 for finding the spectrum of zonal flows in quasigeostrophic β-plane turbulence. This procedure is rooted in the observation made in Sec. II that spectra develop singular boundary layer-like structure in wave number space (consisting of enhanced spectral densities) to compensate for the vanishing of the wave frequency when the wave number in the zonal direction is zero. In the analysis of Ref. 11 the spectrum is inertial. In the present system there is dissipation, however, in a sense to be explained more fully below, the deviation from inertial behavior is weak because $\nu\ll v_D\bar{k}_y$. The procedure of Ref. 11, although heuristic, has been shown from simulation to correctly predict the zonal-flow spectrum. In accordance with the notion of a singular boundary layer in wave number space it balances magnitudes of the wave term and the nonlinearity, equating all wave numbers to the wave number whose direction is normal to the zonal direction.

For TEM the procedure must be interpreted as applying to the evolution equations for $\beta_1(k)$ with $\mathbf{k}'\times\mathbf{z}\cdot\mathbf{k}\to k_yk_x'$, $k_y\to0$, and all remaining wave number dependence evaluated as k_x. To remove the effect of instability we set $\hat{\alpha}=1$. The spectrum is obtained from the evolution equation for β_1, because that is the equation in which the wave term appears. Following the steps just described,
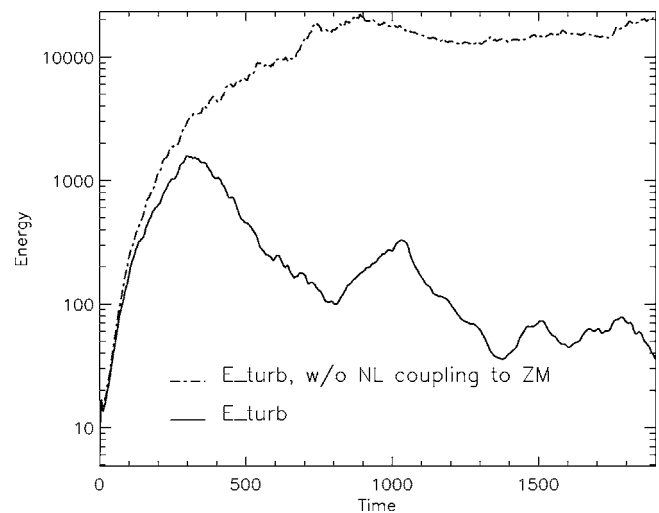

FIG. 4. Total turbulent energy for numerical solution with and without coupling to zonal modes.

$$\omega_1(k)\beta_1(k_x)|_{k_y=0} = \frac{k_y k_x}{[R_1(k) - R_2(k)]}[R_1(k_x)\beta_1(k_x)$$
$$+ R_2(k_x)\beta_2(k_x)]\beta_1(k_x)|_{k_y=0}. \qquad (25)$$

Because both β_1 and β_2 remain in dominant balances, each term on the right hand side of Eq. (25) must balance the wave term, providing spectra for $|\beta_1|^2$ and $|\beta_2|^2$. The balance with the first term yields $\beta_1(k_x) = v_D/\epsilon^{1/2}k_x$. Defining the continuous energy density for β_1 in the usual way as $\int U_1(k_x)dk_x = |\beta_1|^2$, the spectrum is given by

$$U_1(k_x) = \frac{v_D^2}{\epsilon k_x^3}. \qquad (26)$$

The balance with the second term yields $\beta_2(k_x) = \nu/(1 - \epsilon^{1/2})k_x^2$, from which the spectrum of β_2 is found to be

$$U_2(k_x) = \frac{\nu^2}{(1 - \epsilon^{1/2})^2 k_x^5}. \qquad (27)$$

These spectra are steep, particularly the β_2 spectrum, which happens to have the same power law exponent of the quasigeostrophic β-plane spectrum. However, aside from that, what is most telling about these spectra is their relationship to the asymptotic scaling solutions, Eqs. (23) and (24), and the conclusions that can be drawn therefrom.

   We note first that the singular layer spectra of Eqs. (26) and (27) have identical scaling with the nonzonal mode spectra of the asymptotic analysis, i.e., $|\beta_1|^2 \sim v_D^2/\bar{k}^2$ and $|\beta_2|^2 \sim \nu^2/\bar{k}^4$. We now take Eq. (27) as the zonal-mode spectrum that matches to a nonzonal-mode spectrum for β_2 outside the singular layer, and we use it to determine the scaling of the zonal-mode energy in β_2 when the wave number dependence is not resolved. To do this we replace k_x^2 with its dimensional equivalent in the system parameters, $k_x^2 = \nu^2/v_D^2$. We find that the zonal mode energy for β_2 becomes $v_D^2/\bar{k}^2$, exactly as indicated by Eq. (24). This means that the wave number spectra of the singular layer analysis, when averaged over wave number, reproduce the asymptotic scalings extracted from the energy evolution equations. The two approaches are equivalent even though one assumed an inertial range and the other accounted fully for the noninertial distribution of energy sources and sinks. This demonstrates that TEM, although not inertial, is indeed governed by the inertial forces of classic wave-dominated regimes in turbulence, consistent with $\nu \ll v_D \bar{k}_y$.

   Consequently, it is wave physics and the symmetry breaking by anisotropic waves that sets the properties of zonal flows and the spectrum of long wavelength turbulence in TEM. This view connects to fundamental symmetries of the governing equations and unifies the zonal mode physics in TEM with that of other systems. It leads to the placement of TEM turbulence in a dynamical similarity group with quasigeostrophic β-plane turbulence, 3D rotating turbulence, rotating stratified turbulence, and magnetohydrodynamic (MHD).

   Figure 3 shows the time evolution of the energies in zonal and nonzonal wave numbers. Initially there is more energy in nonzonal wave numbers, but eventually the energy

in zonal wave numbers becomes larger. This is consistent with development of the steep spectra of Eqs. (26) and (27) in a region where otherwise the energy tends to roll over and decrease with decreasing wave number. Note that as the zonal mode energy builds up the total energy also adjusts downward from an initially higher, transient saturation level. This is a common feature of zonal mode dynamics, but we emphasize again that here it is caused by the strengthening of a dissipative sink as zonal-mode energy builds.

IV. NONLINEAR ZONAL MODE DAMPING

   The previous sections showed that the TEM system, like other wave-dominated systems with anisotropic frequencies, has strongly anisotropic spectral transfer to zonal modes. At the same time the nonlinearity excites a damped eigenmode that introduces finite-amplitude-induced damping for zonal and nonzonal wave numbers. Here we quantify that damping by specifying the precise mixing of unstable and stable eigenmodes obtained from the saturation analysis of the previous section, and the damping and growth rates intrinsic to these eigenmodes at wave numbers of interest. The basis for calculation of finite-amplitude-induced dissipation is the fluctuation energy, and its time rate of change, which quantifies dissipation rates. The fluctuation energy is a quadratic function of n_k and ϕ_k formulated to include kinetic, potential, and internal energies, and subject to the constraint that the energy is an invariant of the nonlinearities.[22] The latter requires the nonlinearities to vanish when the appropriate moments of Eqs. (3) and (4) are taken to formulate the energy evolution. The above requirements are satisfied when the energy is defined as

$$W = \sum_k E(k) = \sum_k [(1 + k^2 - \epsilon^{1/2})|\phi_k|^2 + \epsilon^{1/2}|n_k|^2]. \qquad (28)$$

Although energy is conserved by the nonlinearities, it is dissipated in the full system, which has dissipative linear terms. The temporal derivative of W yields the net energy into (or out of) the system under the combination of sources and sinks, including the gradient free energy released into unstable wave numbers, and the energy dissipated at stable wave numbers through trapped-electron pitch angle scattering. Taking the derivative of W, and using Eqs. (3) and (4) to express $\dot{n}_k$ and $\dot{\phi}_k$ in terms of the remaining terms, dW/dt can be written

$$\frac{dW}{dt} = \sum_k 2\gamma_k^{nl}E(k), \qquad (29)$$

where γ_k^{nl} is the spectrally resolved energy growth rate, given by

$$\gamma_k^{nl} = \frac{k_y v_D \hat{\alpha}\epsilon^{1/2}\,\mathrm{Im}\langle n_k^*\phi_k\rangle - \nu\epsilon^{1/2}|(n_k - \phi_k)|^2}{(1 + k^2 - \epsilon^{1/2})|\phi_k|^2 + \epsilon^{1/2}|n_k|^2}. \qquad (30)$$

The right-hand side of Eq. (29) comes entirely from the linear terms of Eqs. (3) and (4). The nonlinear terms vanish in the sum over k because W is an invariant. This does not make γ_k^{nl} a linear growth rate. It is nonlinear, or amplitude dependent, because $\langle n_k^*\phi_k\rangle$ and $|(n_k - \phi_k)|^2$ have different values at

finite amplitude than they have at infinitesimal amplitude (where γ_k^{nl} is extremely close to the linear growth rate).

Consider the properties of the nonlinear growth rate. The second term in the numerator arises from collisional detrapping. It is negative or zero, depending on the values of n_k and ϕ_k, but cannot be positive. Instability therefore resides in the first term and occurs when it is positive and larger than the second term. To be positive, $k_y \neq 0$ and $\mathrm{Im}\langle n_k^* \phi_k \rangle > 0$. Note that the first term is proportional to $v_D \hat{\alpha}$, which parameterizes the free energy residing in the density and temperature gradients. Consequently, the gradient free energy is only available to modes with $k_y \neq 0$, and only if $\mathrm{Im}\langle n_k^* \phi_k \rangle > 0$. Zonal modes have $k_y = 0$. They are unable to access the free energy, and cannot be unstable, linearly or nonlinearly. If we set $k_y = 0$ in Eq. (30) we obtain the zonal-mode energy growth rate,

$$\gamma_k^{nl}\big|_{k_y=0} = -\left.\frac{\nu \epsilon^{1/2}|(n_k - \phi_k)|^2}{(1 + k_x^2 - \epsilon^{1/2})|\phi_k|^2 + \epsilon^{1/2}|n_k|^2}\right|_{k_y=0}, \quad (31)$$

which from the previous discussion is negative or zero. Thus although zonal modes have no way of extracting free energy from driving gradients, they are actually damped except when $n_k = \phi_k$.

We turn now to the relationship between n_k and ϕ_k, which governs the zonal mode damping. This relationship is dictated by the eigenmodes, and knowing it allows us to evaluate zonal mode damping. The linear eigenmodes are specified by Eq. (6). Selecting the zonal wave number condition $k_y = 0$, and recalling that $\omega_1 = 0$ for $k_y = 0$, we find that for the unstable eigenmode $R_1 = 1$, or that $n_k = \phi_k$ (which implies that $n_e = 0$). Consequently, the zonal wave number of the unstable eigenmode is marginally stable, the standard expectation. This is consistent with $\omega_1 = 0$. Note that any deviation of the fluctuations from the unstable eigenmode, however slight, introduces nonlinear damping. The unstable eigenmode dominates evolution early in the linear growth phase, making zonal modes undamped initially. However, as the nonlinear eigenmode develops under the excitation of the damped eigenmode, $n_k \neq \phi_k$, and zonal modes become damped.

We evaluate the nonlinear zonal mode damping rate at saturation, substituting into Eq. (31) the values of n_k and ϕ_k consistent with the nonlinear mixing of unstable and damped eigenmodes, as specified in the saturation levels given in Eqs. (24). From the eigenmode decomposition [Eq. (5)], the nonlinear growth rate can be written

$$\begin{aligned}\gamma_k^{nl}\big|_{k_y=0} = &-2\nu\epsilon^{1/2}|\beta_2|^2(R_2-1)^2\,[(1+k_x^2-\epsilon^{1/2})(|\beta_1|^2 \\ &+ |\beta_2|^2 + 2\,\mathrm{Re}\langle\beta_1\beta_2^*\rangle) + \epsilon^{1/2}(|\beta_1|^2 + R_2^2|\beta_2|^2 \\ &+ 2R_2\,\mathrm{Re}\langle\beta_1\beta_2^*\rangle)]^{-1}\big|_{k_y=0}, \end{aligned} \quad (32)$$

where

$$R_2\big|_{k_y=0} = \frac{-(1+k_x^2-\epsilon^{1/2})}{\epsilon^{1/2}} \quad (33)$$

is found by substituting Eq. (14) into Eq. (6). The factor $|\beta_2|^2$ in Eq. (32) underscores the fact that it represents a nonlin-

damping rate, because as a damped eigenmode, β_2 only differs from infinitesimal values if it is excited to finite amplitude by the nonlinearity. For concreteness, let us arbitrarily set to unity the order-unity constants A_{1Z}, A_{2Z}, A_{rZ}, and A_{iZ}. Substituting from Eq. (24), the zonal mode nonlinear damping rate becomes

$$\gamma_k^{nl}\big|_{k_y=0} \approx -\frac{\nu}{1+4\epsilon^{1/2}-\epsilon} \approx -\nu, \quad (34)$$

where the last approximate equality neglects $\epsilon^{1/2}$ as a small parameter and is therefore consistent with the saturation levels given in Eq. (24). We note that the nonlinear zonal mode damping rate is of the same order as the growth rate of the fastest growing mode (and of larger magnitude in this approximation). This is consistent with earlier demonstrations that the instability is saturated by the finite-amplitude-induced damping of zonal modes.

V. CONCLUSIONS

We have undertaken a fully self-consistent spectral study of a system with strong nonadiabatic electron dynamics, and with instability-driven turbulence possessing a prominent zonal-mode component. The system models trapped electron mode turbulence, an important component of the fluctuation spectrum in tokamak discharges. The nonadiabatic electron density is strongly excited at zonal wave numbers, hence the investigation has gone beyond zonal flows to describe the effects of zonal modes in other fluctuation fields. We have explored key features shared with other types of turbulence exhibiting large scale anisotropic structure, including 3D rotating turbulence, rotating stratified turbulence, quasigeostrophic β-plane turbulence, and MHD turbulence.

Zonal modes are a fluctuation component whose spectral density is singularly influenced by the frequency of linear waves. We have shown that spectral transfer is governed by a singular balance in wave number space between the nonlinearity and the wave frequency. Consequently, zonal modes are the nonlinear vestige of the zero-frequency drift wave, preferentially driven by spectral transfer as a consequence of the vanishing of the linear wave frequency at the zonal mode number $k_y = 0$. As such zonal modes are an anisotropic spectrum component expressing the anisotropy of drift wave propagation. The singular balance is enforced in the fluctuation basis that diagonalizes the linear coupling (the eigenmode decomposition).

Because zonal modes are produced by the interplay of linear wave dynamics and nonlinearity, their analysis must account for the possible nonlinear mixing of eigenmodes of the wave dielectric. In TEM turbulence the unstable trapped electron eigenmode is mixed with a second branch whose modes are stable for all wave numbers. Mixing occurs because the stable eigenmode is nonlinearly excited to finite amplitude by the advection of electron density. This nonlinear mixing subjects zonal modes to the robust damping of the stable eigenmode branch. The damping is nonlinear, or finite-amplitude-induced, because it derives from the nonlinear mixing.

Nonlinear damping of zonal modes has two primary consequences. First, it saturates zonal mode excitation, balancing the energy delivered to zonal modes by conservative nonlinear spectral transfer. Second, it is the primary saturation mechanism for the TEM instability when viscous dissipation and collisional density diffusion are smaller than the trapped electron scattering rate. This latter condition, along with the weakly collisional constraint $\nu < v_D k_y$, makes for large Reynolds numbers. However, it does not support conventional large-Reynolds-number saturation via a Kolmogorov-like process involving spectral transfer to viscously damped, small-scale Fourier modes on the unstable eigenmode branch.

This result is created by the confluence of two mechanisms. First, the excitation of the stable eigenmode to finite amplitude opens a potent energy sink that otherwise is not available. Provided the damped eigenmode is excited, this sink dominates the viscous and diffusive sinks, a result verified in simulations. Second, spectral energy transfer strongly favors zonal modes over other modes, making the zonal wave numbers of the damped eigenmode spectrum the dominant energy sink. The predilection of spectral transfer for zonal modes derives from the vanishing of the wave frequency for $k_y = 0$. It is unusually transparent in the nonlinear coupling coefficient of the eigenmode decomposition, which to lowest order in collision strength goes as one over the wave frequency. It is equally salient in simulations. Given these properties, it is not surprising that removing zonal mode coupling dramatically raises the saturation level. Simulations show that the increase in saturation level is an order of magnitude. This type of behavior has long been associated with zonal mode excitation. Although it originates in finite-amplitude-induced dissipation in the present system, this mechanism has not been explored in other systems with zonal modes. The excitation of the geodesic acoustic mode, as observed in experiment,[9] is consistent with finite-amplitude-induced dissipation.

Analysis of this system leads to several other interesting observations. Given the importance of electron density advection at large scale, the spectral transfer that drives zonal mode excitation is partly governed by density fluctuations. Consequently, in looking for bispectral signatures of zonal mode excitation, bispectra with the electron density should be measured. The importance of electron advection at large scales also raises the question of how large scale zonal modes are excited by a nonlinearity known to favor energy transfer to small scales. Recent work shows that while advection of electron density under isotropic conditions indeed produces transfer to small scales, the anisotropy of drift wave propagation leads to inverse energy transfer in wave-dominated turbulence, even though the nonlinearity is isotropic.[17] This process is driven by the same anisotropy that strongly favors coupling to zonal modes, but does not require a zonal mode spectrum component. Hence it plays an important role in building up that component. The inverse spectral transfer process requires excitation of the damped eigenmode. The excitation of the damped eigenmode has interesting consequences for transport. Zonal modes are not a direct player per se, because transport requires $k_y \neq 0$. However, they influence transport through the fluctuation level. A description of particle transport in the TEM system is given elsewhere.

The excitation of zonal modes represents a complex interaction between linear and nonlinear processes. Zonal modes are excited by the spectral transfer of an isotropic nonlinearity, yet they are a prominent anisotropy of the fluctuation spectrum. If zonal modes were governed solely by the nonlinearity, they would be less probable than isotropic modes (because they are confined to a limited volume in wave number space), and not in evidence in visualizations of the turbulence, except as a sporadically appearing fluctuation. However, the anisotropy is rooted in the linear wave terms, dominating the spectrum in the wave-dominated regime where linear terms exceed the nonlinearity. Looking at anisotropic structure as the consequence of a fundamental anisotropy in the linear terms of governing equations raises interesting questions with respect to other types of anisotropy. Consider, for example, the radial streamer, for which $k_r = 0$. This anisotropy resides in the linear growth rate. At saturation the growth rate must be matched by the nonlinearity, and therefore does not represent a situation in which a linear term exceeds the nonlinearity. Is it possible, then, for the streamer to be a prominent part of the spectrum? If not, can the relatively small volume streamers occupy in wave number space allow them to have anything other than a minor impact on transport?

ACKNOWLEDGMENT

[1]D. A. Baver, P. W. Terry, and R. Gatto, Phys. Plasmas **9**, 3318 (2002).
[2]P. W. Terry, R. Gatto, and D. A. Baver, Phys. Rev. Lett. **89**, 205001 (2002).
[3]G. Hammett, M. Beer, W. Dorland, S. C. Cowley, and S. A. Smith, Plasma Phys. Controlled Fusion **35**, 973 (1993).
[4]R. D. Sydora, V. K. Decyk, and J. M. Dawson, Plasma Phys. Controlled Fusion **38**, A281 (1996).
[5]Z. Lin, T. S. Hahm, W. W. Lee, W. M. Tang, and R. B. White, Science **281**, 1935 (1998).
[6]A. Hasegawa and M. Wakatani, Phys. Rev. Lett. **59**, 1581 (1987).
[7]G. R. Tynan, R. A. Moyer, M. J. Burin, and C. Holland, Phys. Plasmas **8**, 2691 (2001).
[8]P. Schoch, Bull. Am. Phys. Soc. **47**, 298 (2002); this work is also discussed briefly in G. R. McKee, R. J. Fonck, M. Jakubowski *et al.*, Phys. Plasmas **10**, 1712 (2003).
[9]M. Jakubowski, R. J. Fonck, and G. R. McKee, Phys. Rev. Lett. **89**, 265003 (2002).
[10]K. Hallatschek and D. Biskamp, Phys. Rev. Lett. **86**, 1223 (2001).
[11]A. Chekhlov, S. Orszag, S. Sukoriansky, B. Galperin, and I. Staroselsky, Physica D **98**, 321 (1996).
[12]F. Waleffe, Phys. Fluids A **5**, 677 (1993).
[13]C. Cambon, L. Jacquin, and J. L. Labrano, Phys. Fluids A **4**, 812 (1992).
[14]A. Hasegawa and K. Mima, Phys. Rev. Lett. **39**, 205 (1977).
[15]L. M. Smith and F. Waleffe, Phys. Fluids **11**, 1608 (1999).
[16]L. M. Smith and F. Waleffe, J. Fluid Mech. **451**, 145 (2002).
[17]P. W. Terry, Phys. Rev. Lett. **93**, 235004 (2004).
[18]Z. Lin, L. Chen, and F. Zonca, Phys. Plasmas **12**, 056125 (2005).
[19]T. S. Hahm, M. A. Beer, Z. Lin, G. W. Hammett, W. W. Lee, and W. M. Tang, Phys. Plasmas **6**, 922 (1999).
[20]P. W. Terry, D. A. Baver, and S. Gupta, Phys. Plasmas **13**, 022307 (2006).
[21]T. Dannert and F. Jenko, Phys. Plasmas **12**, 072309 (2005).
[22]P. W. Terry and W. Horton, Phys. Fluids **25**, 491 (1982).